Author's personal copy

report including the biologic and phenotypic characteristics of the cell line, Cancer 82 (1998) 1416–1417.
[23] S. Osone, H. Hosoi, Y. Kuwahara, Y. Matsumoto, T. Iehara, T. Sugimoto, Fenretinide induces sustained activation of JNK/p38 MAPK and apoptosis in a reactive oxygen species-dependent manner in neuroblastoma cells, Int. J. Cancer 112 (2004) 219–224.
[24] S. Tamura, H. Hosoi, Y. Kuwahara, K. Kikuchi, O. Otabe, M. Izumi, K. Tsuchiya, T. Iehara, T. Gotoh, T. Sugimoto, Induction of apoptosis by an inhibitor of EGFR in neuroblastoma cells, Biochem. Biophys. Res. Commun. 358 (2007) 226–232.
[25] H. Kuroda, T. Sugimoto, K. Ueda, S. Tsuchida, Y. Horii, J. Inazawa, K. Sato, T. Sawada, Different drug sensitivity in two neuroblastoma cell lines established from the same patient before and after chemotherapy, Int. J. Cancer 47 (1991) 732–737.
[26] H. Kuroda, T. Sugimoto, Y. Horii, T. Sawada, Signaling pathway of ciliary neurotrophic factor in human neuroblastoma cell lines, Med. Pediatr. Oncol. 36 (2001) 118–121.
[27] T. Sugimoto, H. Kuroda, Y. Horii, H. Moritake, T. Tanaka, S. Hattori S, Signal transduction pathways through TRK-A and TRK-B receptors in human neuroblastoma cells, Jpn. J. Cancer Res. 92 (2001) 152–160.
[28] F. Saito-Ohara, I. Imoto, J. Inoue, H. Hosoi, A. Nakagawara, T. Sugimoto, J. Inazawa, PPM1D is a potential target for 17q gain in neuroblastoma, Cancer Res. 63 (2003) 1876–1883.
[29] S.L. Cohn, A.D. Pearson, W.B. London, T. Monclair, P.F. Ambros, G.M. Brodeur, A. Faldum, B. Hero, T. Iehara, D. Machin, V. Mosseri, T. Simon, A. Garaventa, V. Castel, K.K. Matthay, The International Neuroblastoma Risk Group (INRG) classification system: an INRG Task Force report, J. Clin. Oncol. 27 (2009) 289–297.
[30] R.C. Seeger, G.M. Brodeur, H. Sather, A. Dalton, S.E. Siegel, K.Y. Wong, D. Hammond, Association of multiple copies of the *N-MYC* oncogene with rapid progression of neuroblastomas, N. Engl. J. Med. 313 (1985) 1111–1116.
[31] G.M. Brodeur, F.A. Hayes, A.A. Green, J.T. Casper, J. Wasson, S. Wallach, R.C. Seeger, Consistent *N-MYC* copy number in simultaneous or consecutive neuroblastoma samples from sixty individual patients, Cancer Res. 47 (1987) 4248–4253.

bjh short report

ATF7IP as a novel *PDGFRB* fusion partner in acute lymphoblastic leukaemia in children

Kenichiro Kobayashi,[1] Kazumasa Mitsui,[2] Hitoshi Ichikawa,[3] Kazuhiko Nakabayashi,[4] Masaki Matsuoka,[2] Yasuko Kojima,[2] Hiroyuki Takahashi,[2] Kazutoshi Iijima,[1] Kaori Ootsubo,[5] Keisuke Oboki,[6] Hajime Okita,[1] Kazuki Yasuda,[7] Hiromi Sakamoto,[3] Kenichiro Hata,[4] Teruhiko Yoshida,[3] Kenji Matsumoto,[8] Nobutaka Kiyokawa[1] and Akira Ohara[2]

[1]Department of Paediatric Haematology and Oncology Research, National Research Institute for Child Health and Development, [2]Department of Paediatrics, Toho Omori Medical Centre, [3]Division of Genetics, National Cancer Centre Research Institute, [4]Department of Maternal-Fetal Biology, National Research Institute for Child Health and Development, [5]SRL Inc., Centre for Molecular Biology and Cytogenetics, [6]Department of Molecular Medical Research, Tokyo Metropolitan Institute of Medical Science, [7]Department of Metabolic Disorder, Diabetes Research Centre, National Centre for Global Health and Medicine, and [8]Department of Allergy and Immunology, National Research Institute for Child Health and Development, Tokyo, Japan

Received 22 December 2013; accepted for publication 29 January 2014

Correspondence: Kenichiro Kobayashi, MD, PhD, Department of Paediatric Haematology and Oncology Research, National Research Institute for Child Health and Development, 2-10-1, Okura, Setagaya-ku, Tokyo 157-8535, Japan.
E-mail: kobayashi-kn@ncchd.go.jp

Summary

We identified *ATF7IP* as a novel *PDGFRB* fusion partner in B-progenitor acute lymphoblastic leukaemia (B-ALL) and showed that B-ALL with *ATF7IP/PDGFRB* translocation is included within the genomic lesions of a Philadelphia chromosome (Ph)-like ALL subgroup. Comprehensive analyses of previous repositories of gene expression data sets disclosed that B-ALL cases with high *PDGFRB* expression level in the context of the Ph-like ALL gene are likely to have a *PDGFRB* translocation. Thus, it is possible that measurement of the *PDGFRB* expression level can be utilized as a screening test for the detection of the cryptic *PDGFRB* translocation, especially within the Ph-like ALL subgroup.

Keywords: *PDGFRB*, *ATF7IP*, acute lymphoblastic leukaemia, Ph-like, screening.

The *PDGFRB* gene (located in 5q33) is a frequent target of chromosomal translocation in a broad spectrum of haematological malignancies, and myeloid neoplasm patients with *PDGFR* translocation are now grouped into a distinct clinical entity of the World Health Organization classification: myeloid neoplasm associated with eosinophilia and *PDGFRA* or *PDGFRB* rearrangement (Tefferi & Vardiman, 2008). Despite increasing evidence of *PDGFR* translocations in haematological malignancy, little is known about *PDGFRB* involvement in B-progenitor acute lymphoblastic leukaemia (B-ALL), presumably due to the limitation of the detection of cryptic *PDGFRB* translocation with conventional diagnostic procedures. Current advances in RNA sequence analysis of B-ALL identified a novel fusion chimera involving *PDGFRB* in

© 2014 John Wiley & Sons Ltd, *British Journal of Haematology*
doi:10.1111/bjh.12834

high-risk B-ALL, namely Philadelphia Chromosome (Ph)-like ALL (Roberts *et al*, 2012). Herein, we report an 8-year-old boy with B-ALL in whom *ATF7IP* was identified as a novel fusion partner in the *PDGFRB* translocation. We examined the molecular characteristics of B-ALL with *PDGFRB* translocation in comparison with previous repositories of gene expression data regarding paediatric B-ALL (Yeoh *et al*, 2002; Roberts *et al*, 2012), and also ascertained that the measurement of *PDGFRB* mRNA expression should be included as a screening test for the detection of such cryptic cytogenetic changes in particular subtypes of ALL, especially Ph-like ALL.

An 8-year-old boy presented in February 2011 with general fatigue of 2 months duration. Physical examination was normal except for pallor and mild hepatomegaly. Laboratory examination showed haemoglobin 47 g/l, platelet count $13{\cdot}1 \times 10^{10}$/l, and leucocyte count $4{\cdot}9 \times 10^{9}$/l (band forms: 30%, segmented neutrophils: 27%, monocytes: 4%, lymphocytes: 23%, and blasts: 16%). A bone marrow (BM) aspirate showed 95% blast cells that stained positive for CD10, CD19, HLA-DR and TdT, but not for myeloperoxidase. Based on these findings, the type of leukaemia of the patient was classified as standard risk B-ALL and he was treated with conventional chemotherapy according to the standard arm of the Tokyo Children's Cancer Study Group Study L99-15 protocol (Manabe *et al*, 2008). He showed good clinical and haematological response with 7 d of prednisolone monotherapy (60 mg/m^2), and blast cells had disappeared from the peripheral blood film on day 8. At the initial diagnosis, a karyotype analysis of blast cells disclosed 45, XY, -7, add (12)(p13). The chromosomal changes involving 12p13 suggested the possibility of t (12;21)(p13;q22); *ETV6/RUNX1* (previously termed *TEL/AML1*), which is known to be the most common translocation in paediatric B-lALL (Jamil *et al*, 2000). The translocation, however, was not detected by either reverse transcription polymerase chain reaction (RT-PCR) or fluorescence *in situ* hybridization (FISH) analysis. Given that the gene locus at 12p13 is frequently involved in chromosomal translocations other than *ETV6*, we performed mRNA sequence analysis (McPherson *et al*, 2011) and identified an in-frame transcript fusing exon 13 of *ATF7IP* with exon 11 of *PDGFRB* (Fig 1A, B). FISH analysis showed cryptic t(5;12)(q33;p13), in which a *ETV6* Dual colour probe (12p13) was fused with a split 3′*PDGFRB* probe (5q33) with a 2-Mb gap (Fig 1C). We also evaluated DNA copy number changes by multiplex ligation-dependent probe amplification analysis (SALSA MLPA KIT P335-A3, MRC-Holland, Amsterdam, the Netherlands), focusing on the common genetic alterations in B-ALL within the *SOX* region, *CRLF2, IKZF1, IL3RA, EBF1, CDKN2A/B, ETV6, BTG1,* and *RB1*. As far as we could determine, no significant copy number alterations except heterozygous deletions within chromosome 7 were present (data not shown). The fusion transcript was readily detected in a BM specimen by quantitative RT-PCR analysis at the time of admission, but its expression decreased with the continuation of chemotherapy. The patient has remained free of disease for 24 months, with the disappearance of the *ATF7IP/PDGFRB* transcripts at the time of this report (Fig 1D, E). To the best of our knowledge, this is the first report showing *ATF7IP* as a fusion partner of *PDGFRB* translocation in haematological malignancy.

ATF7IP has been identified to mediate methylated DNA-binding domain protein 1 (MBD1)-dependent transcriptional repression, recruiting complexes containing SET domain bifurcated 1 (SETDB1) (Fujita *et al*, 2003). Interestingly, a recent analysis suggested that *ATF7IP* facilitates *TERT* and *TERC* expression and is frequently overexpressed in cancer cells (Liu *et al*, 2009). As the N-terminal domain of *ATF7IP* lacked the MBD1 domain, it is likely that the fusion protein does not induce deregulation of *ATF7IP*-mediated transcriptional regulation, but rather is involved in the activation of tyrosine kinase signalling. Indeed, the fusion protein coding ATF7IP locus is predicted to contain a coiled coil structure that is known to contribute to the constitutive activation of kinase and cytokine receptor signalling in *PDGFRB* translocated leukaemia (Lupas *et al*, 1991; Ross & Gilliland, 1999). It is particularly noted that *ATF7IP* fused with *PRGFRB* exon 11, which is the same break point as that of previously reported Ph-like ALL cases with *EBF1/PDGFRB* translocation (Roberts *et al*, 2012).

Fig 1. Detection of *ATF7IP/PDGFRB* fusion gene. (A) Electropherogram of the transcript fusion sequence disclosed in-frame transcript fusing exon 13 of *ATF7IP* with exon 11 of *PDGFRB*. (B) A schematic diagram of the structure of *ATF7IP*, *PDGFRB*, and novel *ATF7IP-PDGFRB* fusion genes. The arrows indicate the breakpoints. Abbreviations: SETB1, SET domain bifurcated 1; MBD1, methylated DNA-binding domain protein 1; Ig, Immunoglobulin-like domain; TM, transmembrane region; TK, tyrosine kinase domain. (C) Fluorescence *in situ* hybridization (FISH) analysis showing chromosomal change of t (5;12)(q33;p13). Signal detection was carried out on metaphases according to the manufacturer's protocols with the following probes: *PDGFRB* Break (KI-10004 KREATECH) and *ETV6* Dual colour Break Apart Rearranged Probe (Vysis Abbott Molecular, Abbot Park, IL). Left upper panel: *PDGFRB* translocation was represented with split signals of 5′*PDGFRB* (broad green arrow) and 3′*PDGFRB* (broad red arrow), respectively. We used *ETV6* Dual colour probes to depict an *ATF7IP* locus, which is located at approximately 2 Mb centromeric from the *ETV6* loci. The resultant translocation of *ATF7IP/PDGFRB* developed fused signals with *ETV6* Dual colour signals (large arrowhead) and 3′*PDGFRB* (broad red arrow) with a 2-Mb gap. Right upper panel: The FITC filter discriminates the presence of split 5′*PDGFRB* (broad green arrow) and the Non-split *PDGFRB* (arrow), respectively. Scale bar, 2 Mb. Bottom: Genomic view of chromosome 12p13 from the UCSC genome Bioinformatics showing the loci of *ETV6* and *ATF7IP*, respectively. (D) Clinical course of the patient with a longitudinal monitoring of the fusion transcript. Top: Percentage of blast cells in a bone marrow specimen. Bottom: The *ATF7IP/PDGFRB* mRNA level was determined by quantitative reverse transcription polymerase chain reaction (RT-PCR). The expression levels were normalized with *ACTB* before calculating the expression ratios. N.D.: the chimeric mRNA was no longer detectable on day 540. (E) RT-PCR analysis of the expression of the *ATF7IP/PDGFRB* fusion transcript (81 bp). *ACTB* confirms the integrity of cDNA (100 bp). Lane 1–2 at diagnosis; lane 3–4 at day 540.

© 2014 John Wiley & Sons Ltd,

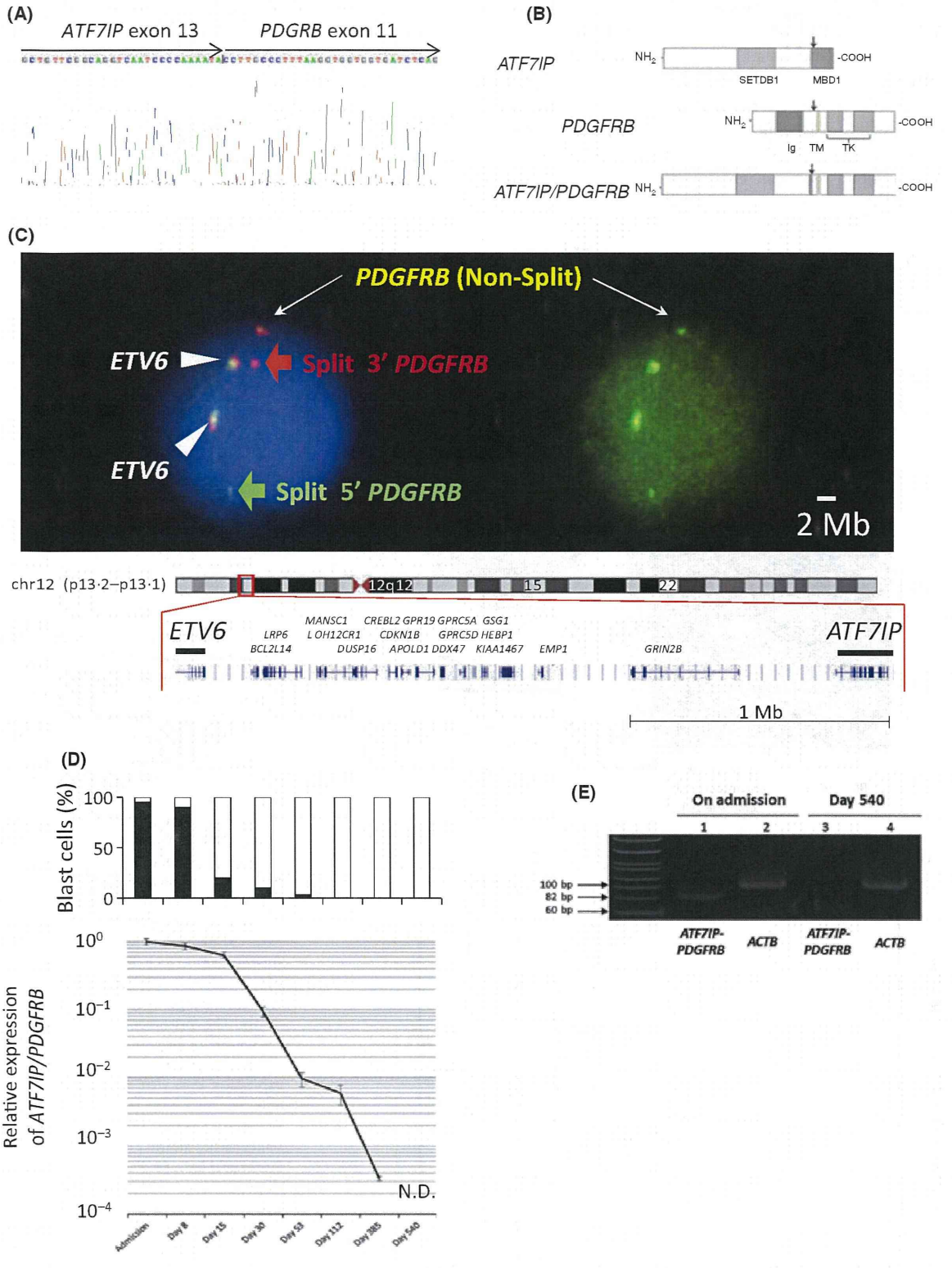
(A)
ATF7IP exon 13
PDGRB exon 11
(B)
ATF7IP
NH2
-COOH
SETDB1
MBD1
PDGFRB
Ig
TM
TK
ATF7IP/PDGFRB
(C)
PDGFRB (Non-Split)
ETV6
Split 3' PDGFRB
ETV6
Split 5' PDGFRB
2 Mb
chr12 (p13·2–p13·1)
12q12
15
22
ETV6
MANSC1
CREBL2 GPR19 GPRC5A GSG1
LRP6
L OH12CR1
CDKN1B
GPRC5D HEBP1
BCL2L14
DUSP16
APOLD1 DDX47
KIAA1467
EMP1
GRIN2B
ATF7IP
1 Mb
(D)
Blast cells (%)
100
50
0
Relative expression of ATF7IP/PDGFRB
10^0
10^-1
10^-2
10^-3
10^-4
N.D.
Admission
Day 8
Day 15
Day 30
Day 53
Day 112
Day 385
Day 540
(E)
On admission
Day 540
1
2
3
4
100 bp
82 bp
60 bp
ATF7IP-PDGFRB
ACTB
ATF7IP-PDGFRB
ACTB

It is strongly suggested that *PDGFRB* translocation in B-ALL comprises a distinct clinical entity, as was shown in acute myeloid leukaemia (Tefferi & Vardiman, 2008). Therefore, we performed microarray analysis of a BM specimen obtained at the time of admission, and compared its expression profiles with public repositories of expression data sets of B-ALL with *BCR-ABL1* translocation (16 cases) and B-ALL without recurrent chromosomal changes (19 cases) (Yeoh *et al*, 2002). By employing gene set enrichment analysis (GSEA) (Subramanian *et al*, 2007), significant enrichment of the *BCR-ABL1* gene expression signature was demonstrated in our case, indicating that B-ALL with *ATF7IP/PDGFRB* translocation can be classified as Ph-like ALL (Fig 2A, B). Interestingly, we found that our case of *ATF7IP/PDGFRB* translocation showed high expression of *PDGFRB* at the mRNA level (Fig 2C). This observation prompted us

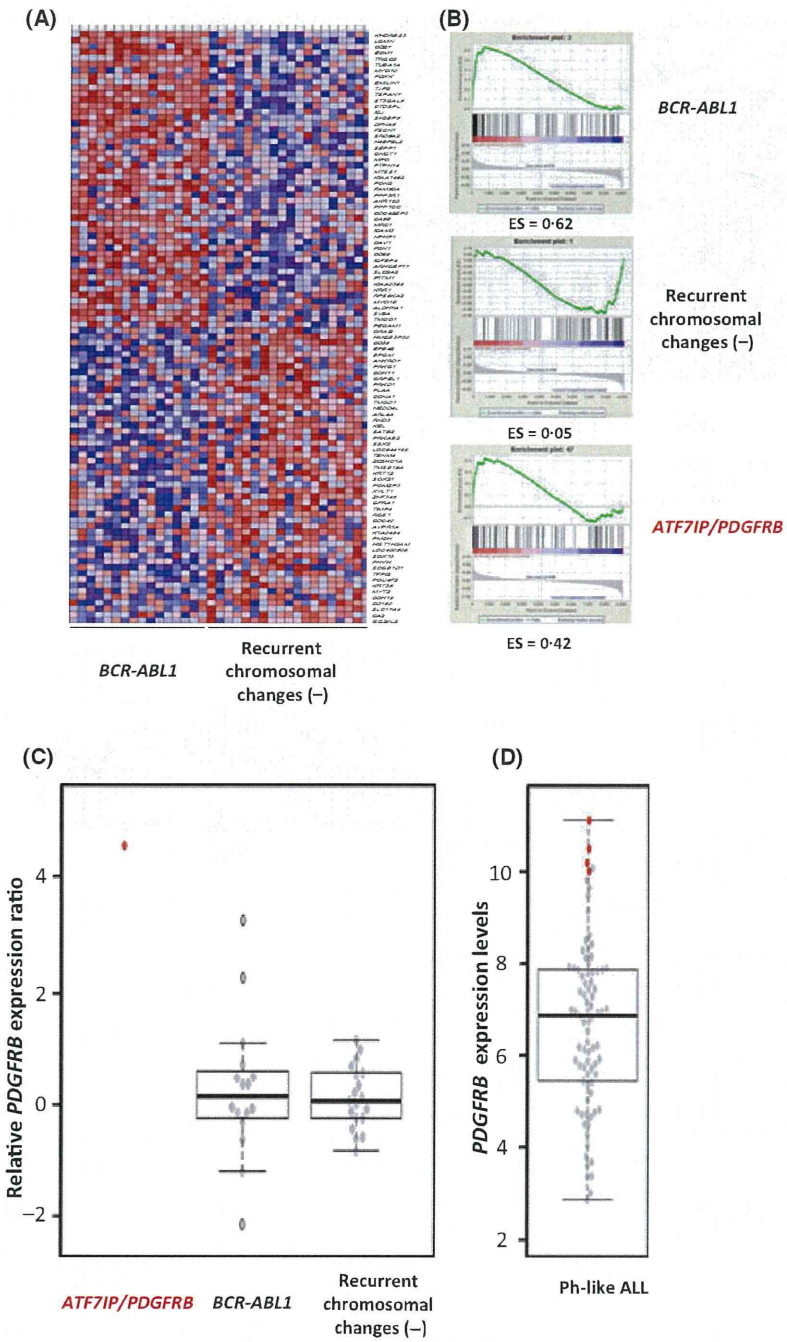

Fig 2. Characterization of gene expression profiles of B-ALL cases with *PDGFRB* translocation. (A–C) Microarray analyses of B-ALL cases with translocation of *ATF7IP/PDGFRB*, *BCR-ABL1* and B-ALL cases without recurrent chromosomal changes. Microarray data set of *ATF7IP/PDGFRB* was obtained from a bone marrow specimen at the time of admission. Expression data sets of both *BCR-ABL1* translocated B-ALL and B-ALL without recurrent chromosomal changes were obtained from those reported by Yeoh *et al* (2002). (A) The top 50 probe sets differentially expressed between *BCR-ABL1* translocated B-ALL and B-ALL without recurrent chromosomal changes are presented as a heat map. (B) Representative GSEA plots of the each subtype of B-ALL i.e. B-ALL with translocation of *BCR-ABL1*, B-ALL without recurrent chromosomal changes and *ATF7IP/PDGFRB* are shown. The enrichment score (ES) is shown at the bottom of the graph. (C) Distribution of the *PDGFRB* expression in B-ALL patients. The expression levels were normalized with *GAPDH* and calculated as the relative *PDGFRB* expression ratio. The ratio in each patient was represented as bee-swarm plots with boxplots. Horizontal bars, median; box, 25–75th percentile; error bars, 10–90th percentile. (D) Distribution of the *PDGFRB* expression within Ph-like ALL patients. Expression data were obtained from the high-risk ALL cohort data set from Children's oncology group (Roberts *et al*, 2012). Four patients with *EBF1/PDGFRB* translocation are indicated as red plots. Data presentation and analyses were performed as in Fig 2C.

© 2014 John Wiley & Sons Ltd, *British Journal of Haematology*

to evaluate another data set of 83 cases of Ph-like ALL (Roberts *et al*, 2012), and found that four cases of *EBF1/PDGFRB* translocation also overexpressed *PDGFRB* (Fig 2D). It is noteworthy that Erben *et al* (2010) reported that screening of *PDGFRA or PDGFRB* translocation is facilitated by quantification of *PDGFRA or PDGFRB* expression in eosinophilia-associated myeloproliferative neoplasms (Erben *et al*, 2010). More importantly, *PDGFRB* overexpression was found in patients with diverse *PDGFRB* translocations irrespective of the fusion partner, i.e. *ETV6-PDGFRB, CCDC6-PDGFRB, GIT2-PDGFRB, MYO18A-PDGFRB and SART3-PDGFRB.* Indeed, precise detection of *PDGFRB* translocations is necessary for not only diagnostic purposes but also for providing tailored therapy, such as tyrosine kinase inhibitor (TKI) treatment (Roberts *et al*, 2012). However, the *PDGFRB* translocation is mostly cryptic and it is difficult to detect with conventional cytogenetic studies, as was shown in our case. We speculate that this might be one of the leading causes of the previous poor recognition of *PDGFRB* translocation in paediatric B-ALL. In view of the limited conventional diagnostic procedures for the detection of *PDGFRB* translocation, we speculate that the quantification of the *PDGFRB* mRNA expression level should be utilized as a simple screening test prior to performing or planning microarray-based comparative genomic hybridization or FISH analysis of the *PDGFRB* locus in specific subtypes of B-ALL, especially in the Ph-like ALL subgroup.

In summary, we have identified *ATF7IP* as a novel fusion partner in *PDGFRB* translocation in a paediatric case of B-ALL. Given the potential suitability of TKI treatment in this particular type of B-ALL (Roberts *et al*, 2012; Lengline *et al*, 2013; Weston *et al*, 2013), detection of cryptic *PDGFRB* translocation is important, especially for patients who would benefit from TKI treatment at the correct clinical phases. Thus, we ascertained the future prospective of measuring *PDGFRB* expression levels as a simple screening test to detect cryptic *PDGFRB* translocation especially in the Ph-like ALL subgroup.

Acknowledgements

This work was supported in part by a Health and Labour Sciences Research Grant (3rd-term comprehensive 10-year strategy for cancer control H22-011), the Grant of the National Centre for Child Health and Development (25-2, 24-16), and the Advanced Research for Medical Products Mining Programme of the National Institute of Biomedical Innovation (NIBIO, 10-41, -42, -43, -44, -45).

Author contributions

K.K. analysed results and wrote the manuscript; K.M., M.M., Y.K., H.T., K.I. analysed results; K.O. performed FISH analyses; H.I., N.K., K.I., K.Y., H.S., K.H., K.M. provided informatics support; T.Y., N.K., A.O. designed the research.

Competing interests

The authors have no competing interests.

References

Erben, P., Gosenca, D., Muller, M.C., Reinhard, J., Score, J., Del Valle, F., Walz, C., Mix, J., Metzgeroth, G., Ernst, T., Haferlach, C., Cross, N.C., Hochhaus, A. & Reiter, A. (2010) Screening for diverse PDGFRA or PDGFRB fusion genes is facilitated by generic quantitative reverse transcriptase polymerase chain reaction analysis. *Haematologica*, **95**, 738–744.

Fujita, N., Watanabe, S., Ichimura, T., Ohkuma, Y., Chiba, T., Saya, H. & Nakao, M. (2003) MCAF mediates MBD1-dependent transcriptional repression. *Molecular and Cellular Biology*, **23**, 2834–2843.

Jamil, A., Theil, K.S., Kahwash, S., Ruymann, F.B. & Klopfenstein, K.J. (2000) TEL/AML-1 fusion gene. its frequency and prognostic significance in childhood acute lymphoblastic leukemia. *Cancer Genetics and Cytogenetics*, **122**, 73–78.

Lengline, E., Beldjord, K., Dombret, H., Soulier, J., Boissel, N. & Clappier, E. (2013) Successful tyrosine kinase inhibitor therapy in a refractory B-cell precursor acute lymphoblastic leukemia with EBF1-PDGFRB fusion. *Haematologica*, **98**, e146–e148.

Liu, L., Ishihara, K., Ichimura, T., Fujita, N., Hino, S., Tomita, S., Watanabe, S., Saitoh, N., Ito, T. & Nakao, M. (2009) MCAF1/AM is involved in Sp1-mediated maintenance of cancer-associated telomerase activity. *The Journal of Biological Chemistry*, **284**, 5165–5174.

Lupas, A., Van Dyke, M. & Stock, J. (1991) Predicting coiled coils from protein sequences. *Science*, **252**, 162–1164.

Manabe, A., Ohara, A., Hasegawa, D., Koh, K., Saito, T., Kiyokawa, N., Kikuchi, A., Takahashi, H., Ikuta, K., Hayashi, Y., Hanada, R. & Tokyo Children's Cancer Study Group (2008) Significance of the complete clearance of peripheral blasts after 7 days of prednisolone treatment in children with acute lymphoblastic leukemia: the Tokyo Children's Cancer Study Group Study L99-15. *Haematologica*, **93**, 1155–1160.

McPherson, A., Hormozdiari, F., Zayed, A., Giuliany, R., Ha, G., Sun, M.G., Griffith, M., Heravi Moussavi, A., Senz, J., Melnyk, N., Pacheco, M., Marra, M.A., Hirst, M., Nielsen, T.O., Sahinalp, S.C., Huntsman, D. & Shah, S.P. (2011) deFuse: an algorithm for gene fusion discovery in tumor RNA-Seq data. *PLOS Computational Biology*, **7**, e1001138.

Roberts, K.G., Morin, R.D., Zhang, J., Hirst, M., Zhao, Y., Su, X., Chen, S.C., Payne-Turner, D., Churchman, M.L., Harvey, R.C., Chen, X., Kasap, C., Yan, C., Becksfort, J., Finney, R.P., Teachey, D.T., Maude, S.L., Tse, K., Moore, R., Jones, S., Mungall, K., Birol, I., Edmonson, M.N., Hu, Y., Buetow, K.E., Chen, I.M., Carroll, W.L., Wei, L., Ma, J., Kleppe, M., Levine, R.L., Garcia-Manero, G., Larsen, E., Shah, N.P., Devidas, M., Reaman, G., Smith, M., Paugh, S.W., Evans, W.E., Grupp, S.A., Jeha, S., Pui, C.H., Gerhard, D.S., Downing, J.R., Willman, C.L., Loh, M., Hunger, S.P., Marra, M.A. & Mullighan, C.G. (2012) Genetic alterations activating kinase and cytokine receptor signaling in high-risk acute lymphoblastic leukemia. *Cancer Cell*, **22**, 153–166.

Ross, T.S. & Gilliland, D.G. (1999) Transforming properties of the Huntingtin interacting protein 1/platelet-derived growth factor beta receptor fusion protein. *The Journal of Biological Chemistry*, **274**, 22328–22336.

Subramanian, A., Kuehn, H., Gould, J., Tamayo, P. & Mesirov, J.P. (2007) GSEA-P: a desktop application for gene set enrichment analysis. *Bioinformatics*, **23**, 3251–3253.

Tefferi, A. & Vardiman, J.W. (2008) Classification and diagnosis of myeloproliferative neoplasms: the 2008 World Health Organization criteria and point-of-care diagnostic algorithms. *Leukemia*, **22**, 14–22.

Weston, B.W., Hayden, M.A., Roberts, K.G., Bowyer, S., Hsu, J., Fedoriw, G., Rao, K.W. & Mullighan, C.G. (2013) Tyrosine kinase inhibitor therapy induces remission in a patient with refractory EBF1-PDGFRB-positive acute lymphoblastic leukemia. *Journal of Clinical Oncology*, **31**, e413–e416.

Yeoh, E.J., Ross, M.E., Shurtleff, S.A., Williams, W.K., Patel, D., Mahfouz, R., Behm, F.G., Raimondi, S.C., Relling, M.V., Patel, A., Cheng, C., Campana, D., Wilkins, D., Zhou, X., Li, J., Liu, H., Pui, C.H., Evans, W.E., Naeve, C., Wong, L. & Downing, J.R. (2002) Classification, subtype discovery, and prediction of outcome in pediatric acute lymphoblastic leukemia by gene expression profiling. *Cancer Cell*, **1**, 133–143.

© 2014 John Wiley & Sons Ltd, *British Journal of Haematology*

Leukemia Research 38 (2014) 42–48

Contents lists available at ScienceDirect

Leukemia Research

journal homepage: www.elsevier.com/locate/leukres

Significance of CD66c expression in childhood acute lymphoblastic leukemia

Nobutaka Kiyokawa[a,*,1], Kazutoshi Iijima[a], Osamu Tomita[a,1], Masashi Miharu[a,b,1], Daisuke Hasegawa[a,c,1], Kenichiro Kobayashi[a], Hajime Okita[a], Michiko Kajiwara[d,1], Hiroyuki Shimada[b,1], Takeshi Inukai[e,1], Atsushi Makimoto[f,1], Takashi Fukushima[g,1], Toru Nanmoku[h], Katsuyoshi Koh[i,1], Atsushi Manabe[c,1], Akira Kikuchi[j,1], Kanji Sugita[e,1], Junichiro Fujimoto[k,1], Yasuhide Hayashi[l,1], Akira Ohara[m,1]

[a] Department of Pediatric Hematology and Oncology Research, National Research Institute for Child Health and Development, Setagaya-ku, Tokyo, Japan
[b] Department of Pediatrics, Keio University School of Medicine, Shinjuku-ku, Tokyo, Japan
[c] Department of Pediatrics, St. Luke's International Hospital, Chuo-ku, Tokyo, Japan
[d] Department of Transfusion Medicine, Medical Hospital, Tokyo Medical and Dental University, Bunkyo-ku, Tokyo, Japan
[e] Department of Pediatrics, School of Medicine, University of Yamanashi, Chuo, Yamanashi, Japan
[f] Division of Pediatric Oncology, National Cancer Center Hospital, Chuo-ku, Tokyo, Japan
[g] Department of Child Health, Faculty of Medicine, University of Tsukuba, Tsukuba, Ibaraki, Japan
[h] Department of Clinical Laboratory, University of Tsukuba Hospital, Tsukuba, Ibaraki, Japan
[i] Department of Hematology/Oncology, Saitama Children's Medical Center, Saitama, Saitama, Japan
[j] Department of Pediatrics, Teikyo University School of Medicine, Itabashi-ku, Tokyo, Japan
[k] Clinical Research Center, National Center for Child Health and Development, Setagaya-ku, Tokyo, Japan
[l] Department of Hematology-Oncology, Gunma Children's Medical Center, Shibukawa, Gunma, Japan
[m] Department of Pediatrics, Toho University Omori Medical Center, Ota-ku, Tokyo, Japan

ARTICLE INFO

Article history:
Received 17 December 2012
Received in revised form
29 September 2013
Accepted 13 October 2013
Available online 22 October 2013

Keywords:
CD66c
Acute lymphoblastic leukemia
CRLF2, Flow cytometry
Genetic abnormality

ABSTRACT

Upon analyzing 696 childhood B-cell precursor acute lymphoblastic leukemia (BCP-ALL) cases, we identified the characteristics of CD66c expression. In addition to the confirmation of strong correlation with *BCR-ABL* positivity and hyperdiploid, we further observed that CD66c is frequently expressed in CRLF2-positive (11/15, $p < 0.01$ against chimeric gene-negative) as well as hypodiploid cases (3/4), whereas it is never expressed in *ETV6-RUNX1*, *MLL-AF4*, *MLL-AF9*, *MLL-ENL*, and *E2A-PBX1*-positive cases. Although the expression of CD66c itself is not directly linked to the prognosis, the accompanying genetic abnormalities are important prognostic factors for BCP-ALL, indicating the importance of CD66c expression in the initial diagnosis of BCP-ALL.

© 2013 Elsevier Ltd. All rights reserved.

1. Introduction

Although most leukemic cells retain the characteristics of their normal counterparts and exhibit commitment to any one of the hematopoietic lineages, they frequently show lineage-uncommitted antigen expression, referred to as "aberrant antigen expression" or "lineage infidelity". For example, both T-cell and B-cell precursor (BCP) acute lymphoblastic leukemia (ALL) cells commonly express aberrant myeloid lineage antigens, while acute myeloid leukemia (AML) cells often exhibit the expression of T- or B-cell lineage antigens. Several possibilities to explain this phenomenon have been postulated, whereas the precise mechanism is still unclear [1–3].

CD66c, also called CEACAM6, KOR-SA3544 antigen, and NCA 90/50, is a heavily glycosylated glycosylphosphatidylinositol (GPI)-anchored protein belonging to the carcinoembryonic antigen family, having two constant Ig-like domains and one variable Ig-like domain [4]. The expression of CD66c is observed only in granulocytes and its precursors among normal hematopoiesis [5], while it is known as the most frequently observed aberrant myeloid

* Corresponding author at: Department of Pediatric Hematology and Oncology Research, National Research Institute for Child Health and Development, 2-10-1, kura, Setagaya-ku, Tokyo 157-8535, Japan. Tel.: +81 3 3417 2496; fax: +81 3 3417 2496.
E-mail address: kiyokawa-n@ncchd.go.jp (N. Kiyokawa).
[1] From the Tokyo Children's Cancer Study Group.

0145-2126/$ – see front matter © 2013 Elsevier Ltd. All rights reserved.
http://dx.doi.org/10.1016/j.leukres.2013.10.008

Table 1
The summary of the characteristics of patients.

	n=	Age (mean ± SD)	Range	Initial WBC/μl (mean ± SD)	Range	Gender (male:female)	NCI risk group (SR:HR)
BCR-ABL	35	8.4 ± 4.1	2–15	141,950.0 ± 202,731.2	1220–881,700	0.60:0.40	0.80:0.20
MLL-chimera	20	5.5 ± 4.8	0–15	233,237.2 ± 336,648.4	3300–1,165,400	0.45:0.55	0.80:0.20
E2A-PBX1	65	6.5 ± 4.5	1–15	39,857.4 ± 44,938.8	1730–223,300	0.52:0.48	0.94:0.06
ETV6-RUNX1	154	4.8 ± 2.8	1–15	26,426.4 ± 73,112.6	1600–788,000	0.56:0.44	1.00:0.00
Neardiploid	267	6.1 ± 4.3	1–17	31,153.1 ± 71,020.0	700–597,000	0.53:0.47	0.96:0.04
CRLF2+	15	7.7 ± 4.7	1–16	95,105.5 ± 134,773.6	4200–368,700	0.60:0.40	0.93:0.07
Hypodiploid	4	7.3 ± 5.0	2–12	10,075.0 ± 7605.4	4900–23,200	0.75:0.25	1.00:0.00
Hyperdiploid	136	4.4 ± 2.9	1–15	14,256.6 ± 27,170.5	1100–259,000	0.54:0.46	1.00:0.00
Total	696	5.6 ± 3.9		39,318.0 ± 102,794.7	700–1,165,400	0.54:0.46	0.96:0.04
Neardiploid							
CD66c+	106	5.7 ± 3.8	1–15	24,402.5 ± 51,598.1	700–379,500	0.54:0.46	0.96:0.04
CD66c-	161	6.3 ± 4.6	1–17	35,555.7 ± 80,919.0	800–597,000	0.53:0.47	0.97:0.03
Hyperdiploid							
CD66c+	91	4.3 ± 2.4	1–12	12,339.3 ± 17,488.1	1100–116,900	0.58:0.42	1.00:0.00
CD66c-	45	4.5 ± 3.9	1–15	18,278.3 ± 40,265.9	1700–259,000	0.44:0.56	1.00:0.00

antigen in B-cell precursor acute lymphoblastic leukemia (BCP-ALL) [6]. CD66c was initially reported to be expressed highly selectively in *BCR-ABL*-positive BCP-ALL, while some *BCR-ABL*-negative cases also express this antigen [7]. Later, it was reported that CD66c was correlated strongly with *ETV6-RUNX1* and *MLL-AF4* negativity and was found at high levels in hyperdiploidy [6,8]. A number of studies to clarify the function of this molecule have been performed, and it has been reported that CD66c is involved in homo- and heterotypic adhesion [9], contributes to Ca2+-mediated signaling [10], and is involved in apoptosis induction [11]. However, the biological significance of this molecule in BCP-ALL is still not fully understood.

In an attempt to explore the significance of the expression of CD66c in BCP-ALL, we precisely characterized the properties of CD66c-positive ALL in a large cohort. In this study, we further extend previous findings and indicate that CD66c expression has a close correlation with a definite set of genetic abnormalities, although it is not limited to a specific one. The detection of CD66c at the initial diagnosis of BCP-ALL is important for the prediction of the presence and absence of certain genetic abnormalities. Although the expression of CD66c itself is not directly linked to the prognosis, the genetic abnormalities accompanying CD66c expression are important prognostic factors for BCP-ALL, and, thus, the genetic findings need to be investigated carefully with the presence of CD66c expression.

2. Materials and methods

2.1. Case selection

A total of 696 patients aged between 1 and 18 years (male: female; 0.54: 0.46) who had been newly diagnosed with BCP-ALL and consecutively enrolled on the Tokyo Children's Cancer Study Group (TCCSG) L16 study from December 2004 to August 2012 were included in this study. The characteristics of patients, including age, initial white blood cell (WBC) count, and NCI risk group, were summarized in Table 1. The investigations were approved by the institutional review boards of all participating institutions. Informed consent was obtained from parents or guardians, and informed assent was obtained from the patients when appropriate given their age and understanding.

Bone marrow (BM) and/or peripheral blood (PB) smears of the patients were stained by standard techniques, and the diagnosis of ALL was made according to the morphologic and cytochemical (myeloperoxidase and nonspecific esterase) criteria of the French-American-British (FAB) classification. All cases had fewer than 3% myeloperoxidase-positive, 3% Sudan black B-positive (myeloid pattern), or 20% butyrate esterase-positive (myeloid pattern) blast cells and no Auer rods. Basically, children with ALL of the mature B-cell type were not enrolled in this trial. BM aspirate or PB was immediately mixed with anti-coagulant and sent by overnight transport to the flow cytometry and fusion transcript laboratories, National Research Institute for Child Health and Development (NCH) and Univ. of Tsukuba, respectively, as part of routine pretreatment studies.

2.2. Flow cytometry

Four-color flow cytometric immunophenotyping with CD45-gating was performed on a flow cytometer (FC500, Beckman-Coulter, Brea, CA). The panel monoclonal antibodies (MoAbs) used for immunophenotyping are presented in Supplementary information. Whole blood samples were stained with various combinations of fluorescein isothiocyanate (FITC)-, phycoerythrin (PE)-, PE-cyanin 5.1 (PC5)-, and PE-cyanine 7 (PC7)-conjugated MoAbs in the presence of electron-coupled dye (ECD)-conjugated CD45, following RBC-lysis treatment. For the detection of cytoplasmic (cyCD3, cyCD22, cyCD79a, cy-μ, and MPO) and nuclear TdT antigens, the cells were permeabilized with the Intraprep Permeabilization reagent kit (Beckman-Coulter). Analysis was done by collecting 10,000 gated list mode events, and selecting an appropriate blast gate for the combination of CD45 and side scatter. An antigen was considered positively expressed when at least 20% of the gated cells expressed that antigen.

DNA contents were examined by Propidium Iodide (PI)-staining. Following RBC-lysis treatment, 2.5×10^5 cells were suspended in phosphate-buffered saline (PBS) containing 0.2% of Triton X-100, 20 μg/ml of PI, and 100 ng/ml of RNase (Sigma–Aldrich, St. Louis, MO). PI fluorescence was collected through a 645-nm dichroic long-pass filter and a 620-nm band-pass filter. Upon appropriate gating, at least 10,000 events were collected and analyzed.

The detection of BCR-ABL protein by flow cytometry was performed by Cytometric Bead Array (CBA) for BCR-ABL protein (Becton Dickinson, BD, Franklin Lakes, NJ) according to manufacturer's instruction.

2.3. Detection of fusion transcripts and conventional cytogenetic analysis

The expression of 8 fusion transcripts: *MLL-AF4*, *MLL-AF9*, *MLL-ENL*, major *BCR-ABL*, minor *bcr-abl*, *ETV6-RUNX1*, *E2A-PBX*, and *SIL-TAL1*, was detected by real-time PCR using appropriate primer sets. Cytogenetic analysis was performed on bone marrow or peripheral blood specimens using standard techniques. At least 20 metaphases were examined for each case. Actual examinations were performed by Special Reference Laboratory (SRL, Tachikawa, Tokyo, Japan). In the present study, we have defined BCP-ALL cases with more than 51 chromosomes or DNA-index > 1.16 (corresponding to 51 chromosomes) as hyperdiploid (high-hyperdiploid) based on the previous reports [12,13]. Similarly, we have defined the cases with fewer than 44 chromosomes [13–15] or DNA-index < 0.95 (corresponding to 43 chromosomes) [16] as hypodiploid (near-haploid, low-hypodiploid and high-hypodiploid). The cases with 44–50 chromosomes have designated as neardiploid.

2.4. Statistical analysis

Statistical analysis was performed by means of Student's *t*-test. A *p*-value less than 0.05 was considered significant. Principal components analysis (PCA) was performed by using TriSP version2.1 developed by Yamasaki H (http://www014.upp.so-net.ne.jp/acremaker/).

3. Results

3.1. Close correlation between CD66c expression and nonrandom genetic abnormalities

We analyzed CD66c expression in 696 unselected patients' specimens with a diagnosis of BCP-ALL and available information on the presence of well-established chimeric genes, including major and minor *BCR-ABL*, *ETV6-RUNX1*, *E2A-PBX1*, *MLL-AF4*, *MLL-AF9*, and *MLL-ENL* and/or cytogenetic findings, including DNA ploidy. As shown in Table 2, CD66c was expressed in 34.9% of all BCP-ALL cases

Table 2
Expression of myeloid antigens in B-cell precursor acute lymphoblastic leukemia.

	CD66c	CD33	CD13	CD15	CD65	CD117
>20% (%)	34.91	21.73	9.20	3.44	2.46	1.62
Number	(243/696)	(151/695)	(64/696)	(23/668)	(17/692)	(11/679)
Mean (%)	23.18	13.53	6.40	3.35	2.80	1.88
SD (%)	31.26	21.85	14.11	8.57	9.59	5.08
Median (%)	4.87	2.58	1.26	0.79	0.70	0.35

and appeared to be most frequently aberrantly expressed in BCP-ALL compared to other myeloid antigens, including CD33 (21.7%), CD13 (9.2%), CD15 (3.4%), CD65 (2.5%), and CD117 (1.6%).

Consistent with previous reports, CD66c expression showed a close correlation with nonrandom genetic abnormalities and was expressed only in *BCR-ABL*-positive (91.4%, 32/35) or specific chimeric gene-negative cases (50.0%, 211/422), while none of the *ETV6-RUNX1*-positive cases expressed CD66c (Fig. 1A). In addition, not only the *MLL-AF4*-positive cases, but also *MLL-AF9* and *MLL-ENL*-positive cases were negative for CD66c. Furthermore, it is noteworthy that none of the *E2A-PBX1*-positive cases expressed CD66c.

3.2. High rate expression of CD66c in CRLF2-positive and hyperdiploid cases

Next, we further analyzed CD66c expression in BCP-ALL cases without specific chimeric genes (Fig. 1B). The chimeric gene-negative BCP-ALL cases can be subdivided into near-, hyper-, and hypodiploid based on the number of chromosomes. The abnormalities in chromosome number have been shown to have prognostic significance in BCP-ALL and hyperdiploid ALL (more than 51 chromosomes) exhibit a superior outcome [12,13], whereas hypodiploid ALL (fewer than 44 chromosomes) is characterized by extremely poor outcomes when compared with their nonhyperdiploid counterparts (44–50 chromosomes) [13–15]. As shown in Fig. 1B, hyperdiploid cases exhibited high frequency of CD66c expression (66.9%, 91/136). Interestingly, although the number of cases was small, three out of four hypodiploid cases were positive for CD66c.

In our study, we examined the expression of CRLF2 using specific monoclonal antibody retrospectively and prospectively, and found 15 CRLF2-positive cases in the neardiploid cases (2.2% in our total cohort). As shown in Fig. 1B, CRLF2-positive cases exhibited a significantly high frequency of CD66c-expression and 73.3% (11/15) were CD66c-positive. No significant difference was observed between hyperdiploid and CRLF2-positive cases in CD66c-expression. In contrast, the remaining neardiploid cases exhibited less frequent CD66c-expression (39.7%, 106/267).

3.3. Correlation between CD66c expression and that of other myeloid antigens and CD21/CD27 expression

It was reported that the expression of myeloid antigens tended to be mutually exclusive with CD66c [6]. Therefore, we next examined the correlation between the expression of CD66c and other myeloid antigens. As presented above, BCP-ALL cases possessing specific chimeric genes except *BCR-ABL* never express CD66c. Since it was also reported that *ETV6-RUNX1*-positive ALL frequently expressed CD33 and CD13 [17], ALLs expressing these two antigens should be enriched in CD66c-negative/neardiploid cases. Therefore, we compared *BCR-ABL*-positive and chimeric gene-negative cases by excluding BCP-ALL cases possessing other specific chimeric genes from this analysis.

As shown in Fig. 2A and B, the expression of CD33 and CD13 was concentrated in *BCR-ABL*-positive and neardiploid cases. As described above, the vast majority of BCR-ABL-positive cases expressed CD66c and they exhibited a higher frequency of both CD33 (37.5%, 12/32) and CD13 (18.8%, 6/32) expression compared to CD66c-positive cases with neardiploid and hyperdiploid states. In contrast, although we excluded *ETV6-RUNX1*-positive cases from the analysis, neardiploid/CD66c-negative cases still exhibited a significantly higher expression of CD33 (23.6%, 38/161) compared to neardiploid/CD66c-positive (17.9%, 19/106) and hyperdiploid/CD66c-negative (4.6%, 2/44) cases. In CRLF2-positive/CD66c-positive cases, frequent expression of CD33 (36.4%, 4/11) but not CD13 was observed. Since positivity for CD15 and CD65 was low in BCP-ALL, with the exception of *MLL*-related chimeric gene-positive cases [18], no significant differences in the expression of these antigens depending on CD66c expression were observed (data not shown).

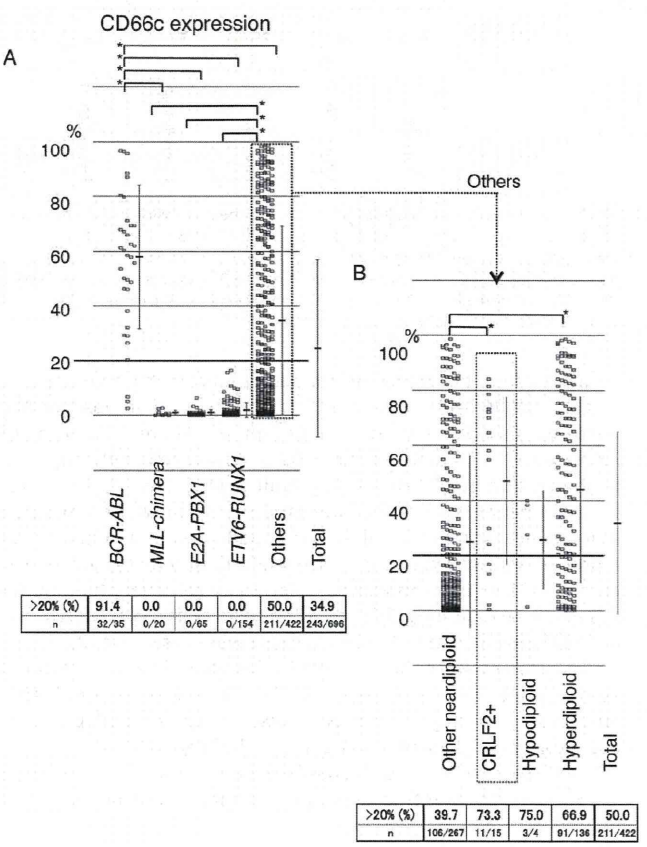

Fig. 1. Correlation between percentage CD66c positivity and acute lymphoblastic leukemia (ALL) genotype categories. (A) CD66c positivity (percentage) of B-cell precursor ALL ($n = 696$) was plotted on a scattergram categorized by the presence of well-known chimeric genes. Percentage of CD66c-positive cases (more than 20% expression in blasts) in each genotype group is listed below. (B) CD66c positivity (percentage) of B-cell precursor ALL without chimeric genes listed above ($n = 422$) was further subclassified based on the DNA-ploidy and CRLF2 expression and presented as in (A). $^*p < 0.01$, using Student's t-test.